

PHASE TRANSFORMATION, STRUCTURE AND MAGNETIC PROPERTIES OF $\text{Nd}_{9.4}\text{Pr}_{0.6}\text{Fe}_{\text{bal}}\text{Ti}_x\text{C}_x\text{Co}_6\text{Ga}_{0.5}\text{B}_6$ RIBBONS PREPARED BY MELT-SPINNING METHOD

RAHIM SABBAGHIZADEH^{a,*}, MANSOR HASHIM^{a,b}, R.GHOLAMIPOUR^c, GH.BAHMANROKH^a, S.KANAGESAN^a

^a*Advanced Material and Nanotechnology Laboratory, Institute of Advanced Technology (ITMA), University Putra Malaysia, 43400 UPM Serdang, Selangor, Malaysia*

^b*Physics Department, Faculty of Science, Universiti Putra Malaysia, 43400 Serdang, Selangor, Malaysia*

^c*Advanced Materials and Renewal Energy Dep., Iran Research Organization for Science and Technology (IROST), Tehran, Iran*

The effect of Carbon and Titanium additions on the phase constitution, microstructures and the magnetic properties of Nd–Fe–B isotropic nanocomposite processed from $\text{Nd}_{9.4}\text{Pr}_{0.6}\text{Fe}_{\text{bal}}\text{Co}_6\text{B}_6\text{Ga}_{0.5}\text{Ti}_x\text{C}_x$ ($x=0, 3, 6$) ribbons has been investigated. As-spun ribbons were examined by using X-ray diffractometry (XRD) and differential scanning calorimetry (DSC). Optimally quenched and annealed $\text{Nd}_{9.4}\text{Pr}_{0.6}\text{Fe}_{\text{bal}}\text{Co}_6\text{B}_6\text{Ga}_{0.5}\text{Ti}_x\text{C}_x$ ($x=0, 3, 6$) ribbons at 750 °C for 10 minutes, which was composed of $\text{Nd}_2\text{Fe}_{14}\text{B}$ grains separated by α -Fe grain boundary phase, shows addition of Ti suppresses formation of primary Fe and promotes formation of ferromagnetic iron-borides. Carbon addition is effective for grain refinement and suppression of unfavourable formation of TiB_2 ; resulting in improvement of magnetic properties. The results show that Titanium and Carbon additions enhance the glass forming ability and increase the crystallization temperature. XRD results of annealed ribbons indicate that Ti and C react to form TiC. The grain size was substantially refined by the addition of Ti due to the formation of Ti-enriched amorphous grain boundaries. The XRD and Atomic force microscope (AFM) technique results confirm that grains are in the size of less than 70 nm. Furthermore, addition of C enhanced the enrichment of Ti in the grain boundary phase, which led to the increase of the coercivity and the maximum energy product.

(Received August 5, 2013; Accepted November 29, 2013)

Keywords: Nanocomposite magnet; Nd–Fe–B magnets; Melt spinning

1. Introduction

Nanocrystalline two-phase composite magnets consisting of a fine mixture of grains of the soft phase uniformly distributed in the magnetically hard and soft phases have attracted much attention for potential permanent magnet development [1]. The first one-dimensional model to explain the superior magnetic behavior of the nanocomposite magnet was reported by Kneller and Hawig [2,3] who predicted that the highest coercivity can be achieved by the exchange coupling force when the size of soft magnetic phase is twice as big as the domain wall width of the hard magnetic phase (~20 nm). Magnetic characters of the nanocomposite magnets are influenced sensitively by their microstructures such as the volume ratio between hard and soft magnetic phases, the grain sizes and their uniform distribution [4]. In addition, it was found that the alloy

*Corresponding author: r.h.sabba@gmail.com

composition of the $\text{Nd}_2\text{Fe}_{14}\text{B}/\alpha\text{-Fe}$ nanocomposites could be optimized to ease the production of amorphous ribbons by melt spinning. Furthermore, the size and volume fraction of $\alpha\text{-Fe}$ and $\text{Nd}_2\text{Fe}_{14}\text{B}$ can be manipulated by thermal processing and by elemental substitution, leading to the increase of the magnetic properties, e.g., B_r and $(BH)_{\max}$, of the fully processed materials [5]. Titanium is known as a suppressing agent for growth of dendrites of $\alpha\text{-Fe}$ in Nd-Fe-B alloys [6]. The appropriate addition of Ti leads to an increase of coercivity in rapid quenched Nd-Fe-B alloys with low levels of Nd and B [7]. The addition of Ti and C was found to be particularly effective in increasing the coercivity without sacrificing remanence [8]. The changes of the grain growth kinetics by C and Ti additions were also reported. However, there is little understanding on the underlying mechanism of Ti and C addition in improving the magnetic properties of the $\text{Nd}_2\text{Fe}_{14}\text{B}/\alpha\text{-Fe}$ nanocomposite magnets [9]. In the present work, the effects of the addition, Ti and C, on the structure and magnetic properties of melt spun $\text{Nd}_{9.4}\text{Pr}_{0.6}\text{Fe}_{\text{bal}}\text{Co}_6\text{B}_6\text{Ga}_{0.5}\text{Ti}_x\text{C}_x$ ($x=0, 3, 6$) ribbon, which heat treatment at 750°C for 10 minutes, have been investigated.

2. Experimental procedure

Ingots of $\text{Nd}_{9.4}\text{Pr}_{0.6}\text{Fe}_{\text{bal}}\text{Co}_6\text{B}_6\text{Ga}_{0.5}\text{Ti}_x\text{C}_x$ ($x=0, 3, 6$) alloys were prepared from Fe, Nd, and Ti metals with purity greater than 99.5% and commercial-grade Fe-B and Fe-C alloys by induction melting in an argon gas atmosphere and casting onto a chilled hearth. These ingots were initially alloyed by arc melting for several times to obtain homogeneous composition, and then melt spun at a wheel speed of 40 m/s. The thickness of the ribbons was about 35 μm . The chamber Argon pressure was 950mbar and the ejection pressure was 0.3 bars, and the orifice diameter of the quartz tube was 0.6mm. The as-spun ribbons were sealed in a quartz tube under 4.5×10^{-4} mbar vacuum and afterwards were isothermally annealed at 750°C for 10 minutes to optimize their hard magnetic properties then cooled in water. The ribbons were identified to be completely amorphous by XRD analysis. The magnetic transformation and crystallization behaviors were detected by differential thermal analysis (DTA), and demagnetization curves were measured by using a vibrating sample magnetometer (VSM) after magnetizing the ribbons with a pulsed magnetic field of at least 1.5 T. The atomic force microscope (AFM) was utilized to study microstructure of annealed ribbons.

3. Result and discussion

Fig.1 demonstrates x-ray diffraction patterns of as-spun ribbons for different amount of titanium and carbon. It shows that in $x=0$ ribbon, $\alpha\text{-Fe}$ phase is appearance but ribbons consist of Ti and C additions have amorphous structures. As mentioned before the wheel speed is constant and because of the straight relation between cooling rate and wheel speed it can be concluded that the cooling rate in our experiment is constant so formation of amorphous structures is due to change of critical cooling rate necessary to form an amorphous structure from the melt. On the other hand a mixture of titanium and carbon enhances glass forming ability (GFA) in $\text{Nd}_2\text{Fe}_{14}\text{B}$ melts by lowering the critical cooling rate.

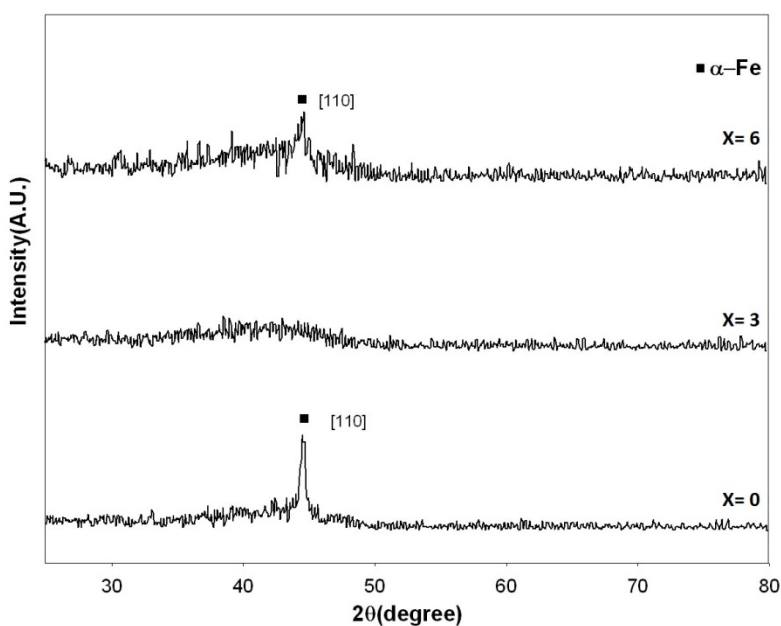


Fig. 1 X-ray diffraction patterns of as-spun ribbons for different compositions.

Fig. 2 shows the DSC scans for crystallization of all the compositions. For all of them there is only one exothermic peak which means the prior precipitation of α -Fe was inhibited and crystallization of both α -Fe and $\text{Nd}_2\text{Fe}_{14}\text{B}$ occur simultaneously. It is also noticeable that addition of Ti and C increases the crystallization temperature up to $x=3$ and then it decreases. Besides, these additives narrow the range between the crystallization and transformation temperature. Enhancement of crystallization temperature up to $x=3$ can be explained by the free volume model [10]. According to this model the amount of free volume necessary for diffusion decreases because of changes in the short range order of local structure of the melt due to addition of Ti and C. Also its descent after $x=3$ may arise from small TiC particles that segregates during crystallization at $x=6$ which act as heterogeneous sites for amorphous phase crystallization and consequently decrease the crystallization temperature.

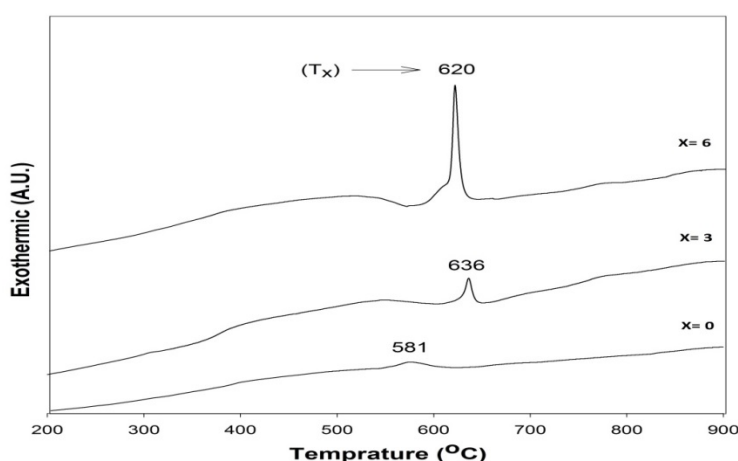


Fig. 2 DSC scans of $\text{Nd}_{9.4}\text{Pr}_{0.6}\text{Fe}_{61}\text{Co}_6\text{B}_6\text{Ga}_{0.5}\text{Ti}_x\text{C}_x$ ($x=0, 3, 6$)

Fig.3 shows powder X-ray diffraction patterns of the annealed ribbons after thermal treatment at 750°C . It is found that the $x=0$ ribbons consist of the hard magnetic 2:14:1 phase and a soft magnetic α -Fe phase but in (Ti,C)-doped ribbons TiC has precipitated as well. Previous research have shown that in a Nd-Fe-B-Ti-C system, the balance of free energy leads to formation

of the most stable phases such as TiC and $\text{Nd}_2\text{Fe}_{14}\text{B}$ [18]. The average grain sizes of annealed ribbons were deduced from Scherrer's method of XRD. The results are shown in Fig 4, the grain size of the α -Fe crystal is substantially decreased by the addition of Ti, and generally carbides are famous for modification of grain growth [11].

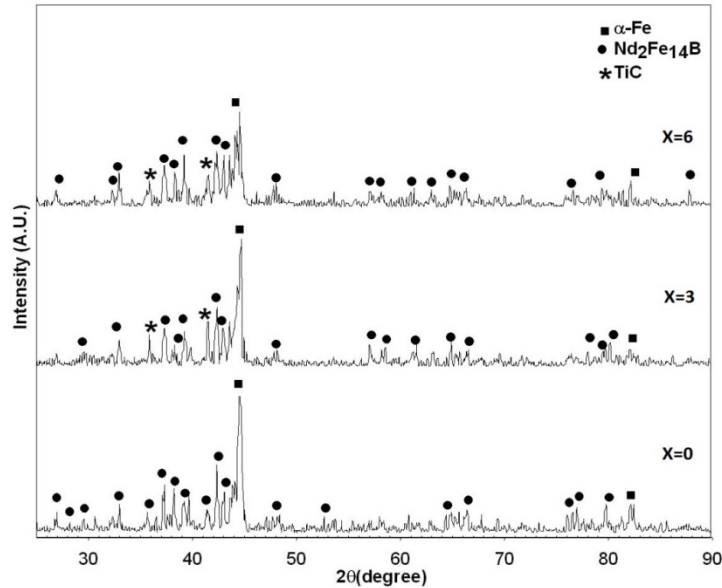


Fig. 3 XRD patterns of ribbons after thermal treatment at 750°C for 10 minutes.

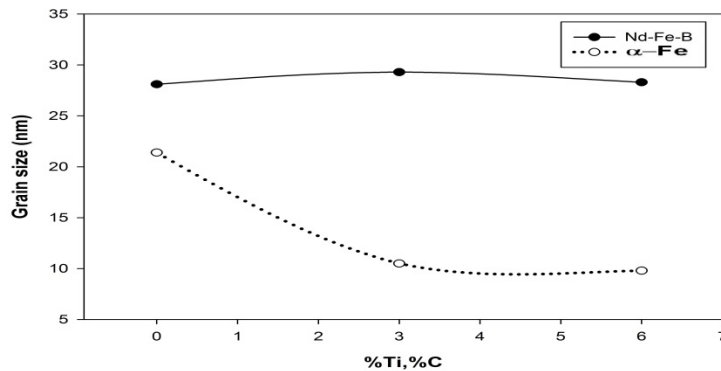


Fig. 4 grain sizes of $\text{Nd}_{9.4}\text{Pr}_{0.6}\text{Fe}_x\text{Co}_6\text{B}_6\text{Ga}_{0.5}\text{Ti}_x\text{C}_x$ ($x=0, 3, 6$) annealed ribbons At 750°C (for 10 minutes) annealing temperature.

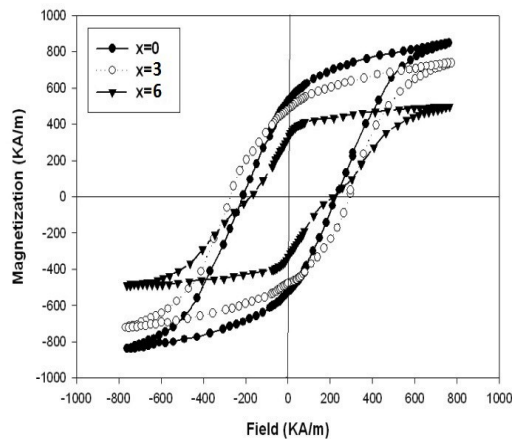
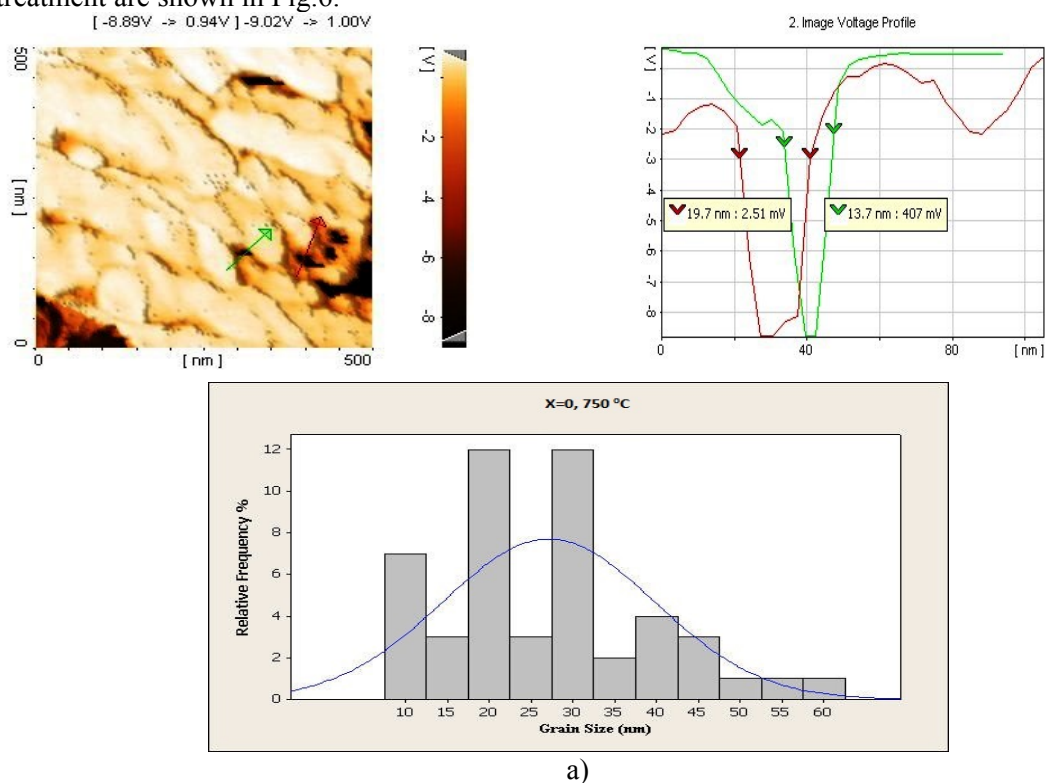


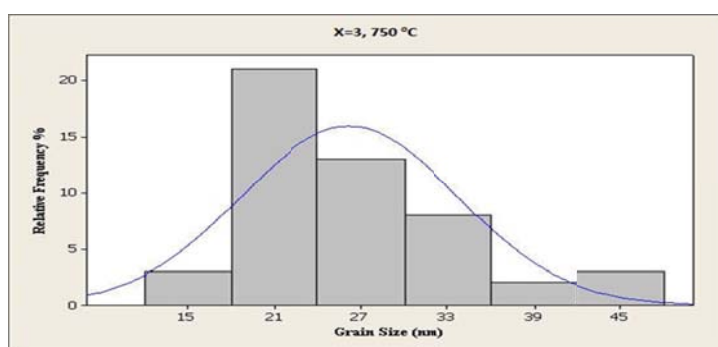
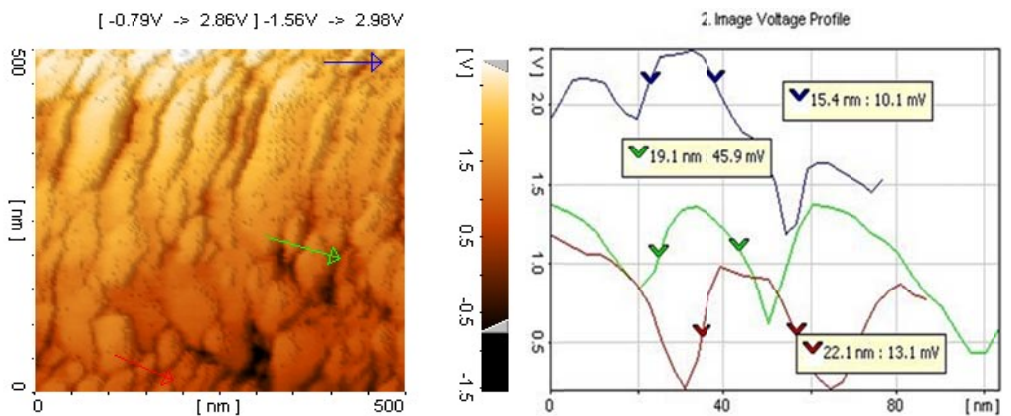
Fig. 5 Hysteresis loops of $\text{Nd}_{9.4}\text{Pr}_{0.6}\text{Fe}_x\text{Co}_6\text{B}_6\text{Ga}_{0.5}\text{Ti}_x\text{C}_x$ ($x=0, 3, 6$) at 750°C annealing temperature for 10 minutes.

Table 1 Magnetic properties of $Nd_{9.4}Pr_{0.6}Fe_{bal}Co_6B_6Ga_{0.5}Ti_xC_x$ ($x=0, 3, 6$) annealed ribbons at 750°C annealing temperature for 10 minutes.

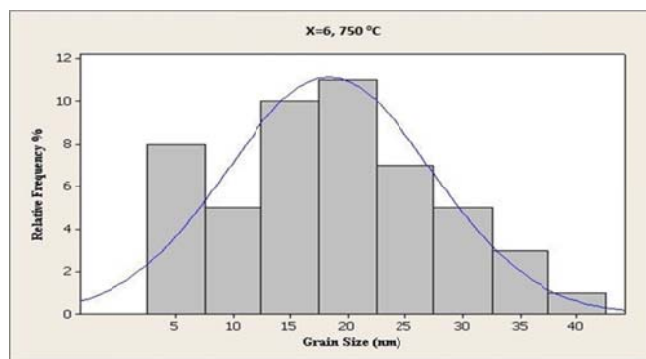
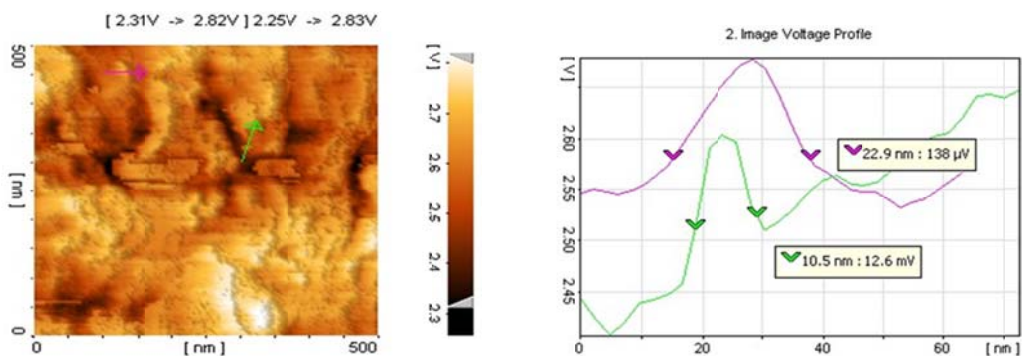
Composition	$(BH)_{max}(KJ/m^3)$	H(KA/m)	$B_r(T)$
$Nd_{9.4}Pr_{0.6}Fe_{bal}Co_6B_6Ga_{0.5}$	23.36	157	0.66
$Nd_{9.4}Pr_{0.6}Fe_{bal}Co_6B_6Ga_{0.5}Ti_3C_3$	28.88	198	0.61
$Nd_{9.4}Pr_{0.6}Fe_{bal}Co_6B_6Ga_{0.5}Ti_6C_6$	19.72	143	0.44

Stable precipitates suppress enlargement of grains and limit their growth. The effect of these precipitates when they are more distributed and in great volume fraction becomes stronger. The grain sizes of $Nd_2Fe_{14}B$ have not changed drastically during annealing at different temperatures which shows that TiC particles do not have any effect on grain growth of the hard magnetic phase. As revealed by AFM (Fig. 5), the grain-size distribution for $x=0$ ribbons, annealed at 750°C for 10 minutes (Fig.5 (a)), is in the range of 10-60(nm). For $x=3$ (Fig.5 (b)) with the same annealing conditions the range changes to 15-45 (nm), and for $x=6$ (Fig.5 (c)) again with similar heat treatment conditions it is 5-40(nm). The results show that the addition of titanium and carbon makes the grain size smaller; however 3% (atomic percent) of Ti and 3% (atomic percent) of C is more favourable because of a better homogeneity of the grain size. Magnetic properties of annealed ribbons were measured by an amplitude gradient force magnetometer (AGFM) with maximum applied field of 1.5 Tesla. Hysteresis loops of the alloys after optimal annealing heat treatment are shown in Fig.6.





b)



c)

Fig. 6 Atomic force microscope (AFM) topography and grain size distribution of (a) $x=0$, (b) $x=3$, (c) $x=6$ Annealed ribbons at 750°C for 10 minutes.

The calculated data are summarized in Table 1 which demonstrates the dependence of magnetic properties on Ti and C content and temperature of annealing. As can be seen the best magnetic properties obtain at 3% (atomic percent) of Ti and 3% (atomic percent) of C addition, which shows the optimum amount of additives. As discussed before Ti and C form TiC particles which precipitate in grain boundaries and suppress grain growth of α -Fe, therefore the maximum energy product (BH_{max}) which is sensitive to exchange coupling and grain size firstly by addition of 3% (atomic percent) of Ti and 3% (atomic percent) of C enhances due to reduction of grain size of α -Fe, on the other hand refinement of soft grains leads to increase of interface between soft and hard grains. Therefore, exchange coupling improves and the greater the volume fraction of TiC the weaker the effective contact between hard and soft grains that leads to weakening of exchange coupling at 6% (atomic percent) of Ti and 6% (atomic percent) of C addition. Coercivity of the ribbons increases to 3% (atomic percent) of Ti and 3% (atomic percent) of C addition and then it decreases. TiC particles and extended grain boundaries (due to grain refinement) play a pinning role to propagate reverse magnetization. Probably, according to AFM results, the greater value of TiC grain size from the distribution of these particles is sufficient to lead to increase of coercivity. Induction remanence (B_r) reduces by addition of Ti and C addition due to non-magnetic behavior of additives elements.

4. Conclusion

The effect of grain size on the magnetization reversal has been studied experimentally for nanostructured two phase ribbons magnet. The glass forming ability increases by addition of Ti and C because of enhancement of inter atomic reactions leading to the ability to produce more homogeneous amorphous materials. Furthermore, simultaneous crystallization temperature of α -Fe and $Nd_2Fe_{14}B$ increases by addition of Ti and C. Addition of C enhances the saturation magnetization as well as the remanence by scavenging Ti from the $Nd_2Fe_{14}B$ grains due to the formation of TiC in the α -Fe grain boundary phase. The best magnetic properties are obtained from the samples which contain 3 at% Ti and 3 at% C.

Acknowledgements

The authors would like to thank Mr Moraddeh for valuable assistance in this experience.

References

- [1] R. Sabbaghizadeh, M. Hashim and S. Moraddeh, Dependence of Microstructure and Magnetic Properties of (Nd,Pr)-(Fe,Ti,C)-B Melt-Spun Ribbon on Quenching Wheel Speed, *Electron. Mater.Lett*, 9 337-340(2013).
- [2] W. Chang, J. Chang, H. Chang, S. Chen, *Physica B: Condensed Matter*, **327**, 296 (2003).
- [3] B. Cui, X. Sun, W. Liu, D. Geng, Z. Yang, Z. Zhang, *Journal of alloys and compounds*, **302** 281 (2000).
- [4] R. Sabbaghizadeh, M. Hashim, Effects of Heat Treatment on the Magnetic Properties of Melt-Spun $Nd_6Pr_1Fe_76B_{12}Ti_4C_1Co_3$ Nanocomposite Ribbons, *Electron. Mater.Lett*, 9 115-118(2013)
- [5] E.F. Kneller and R. Hawig, *IEEE Trans. Magn.*, **27**, 3588 (1991).
- [6] R. Skomski, *Journal of Applied Physics*, **76**, 7059 (1994).
- [7] S. Hirosawa, H. Kanekiyo, T. Miyoshi, *Journal of magnetism and magnetic materials*, **281**, 58 (2004).
- [8] T. Schrefl, J. Fidler and H. Kronmüller, *Phys• Rev.* **B49**, 6100 (1994).
- [9] J. Jakubowicz, M. Jurczyk, *Journal of alloys and compounds*, **269**, 284 (1998).
- [10] D. Branagan, R. McCallum, *Journal of alloys and compounds*, **230**, 67 (1995).
- [11] Z. Chen, Y. Zhang, G.C. Hadjipanayis, Q. Chen, B. Ma, *Journal of magnetism and magnetic materials*, **206**, 8 (1999).

- [12] G.C. Hadjipanayis, *Journal of magnetism and magnetic materials*, **200**, 373 (1999).
- [13] D. Scott, B. Ma, Y. Liang, C. Bounds, *Journal of Applied Physics*, **79**, 4830 (1996).
- [14] W. Chang, S. Wu, B. Ma, C. Bounds, *Journal of magnetism and magnetic materials*, **167**, 65 (1997).
- [15] K.H.J. Buschow, in: K.H.J. Buschow (Ed.), *Handbook of Magnetic Materials* **10**, 46 (1997)
- [16] D. Branagan, R. McCallum, *Journal of alloys and compounds*, **218**, 143 (1995).